IET Generation, Transmission & Distribution

WILEY

The Institution of Engineering and Technology

CASE STUDY OPEN ACCESS

Resilience Analysis of Extensive Meshed Distribution Network to Supply Feeder Outages

Vit Krcal[1] | Jan Koudelka[1,2] | Matej Vrtal[1] | David Topolanek[1] | Petr Toman[1]

[1]Faculty of Electrical Engineering and Communication, Department of Electrical Power Engineering, Brno University of Technology, Brno, Czechia | [2]Faculty of Mechanical Engineering, Jan Evangelista Purkyne University in Usti nad Labem, Usti nad Labem, Czechia

Correspondence: Vit Krcal (vit.krcal@vut.cz)

Received: 9 May 2025 | **Revised:** 7 August 2025 | **Accepted:** 9 September 2025

Funding: This publication was supported by the project "The Energy Conversion and Storage," funded as project No. CZ.02.01.01/00/22_008/0004617 by Programme Johannes Amos Comenius, call Excellent Research.

ABSTRACT

Resilience assessment is also relevant for highly reliable power systems, such as meshed networks. The paper deals with resilience of an urban dense-meshed low voltage network to supply feeder outages and subsequent cascading failures. Presented resilience analysis evaluates the amount of preserved load during multiple feeder outages. The simulations account for a time-span of 1 year of network operation with regard to load variations. Based on disturbances simulation results, the weakest elements of the network are identified. To increase resilience, corrective measures are proposed and incorporated into the simulations. Resilience improvements of applied measures are evaluated and discussed.

1 | Introduction

A reliable electricity supply has become essential for modern society, extending beyond critical infrastructure to affect nearly all human activities. Recent trends in both research and practical power system operation emphasize maintaining supply even under extreme adverse conditions. This need arises from the increasing integration of volatile renewable energy sources and the growing frequency of natural disasters that damage infrastructure, disrupt supply, and incur significant economic costs. Consequently, the concepts of reliability and resilience have gained prominence. While reliability is well established with standardized evaluation methods and indicators, resilience lacks universally accepted metrics and standards.

In the context of electricity networks, resilience refers to the ability of power systems to prepare for, adapt to, withstand, and recover rapidly from major disturbances, whether intentional or naturally occurring [1]. Various studies have provided comprehensive insights into resilience, for example [2, 3]. There is a general agreement that resilience primarily addresses high-impact, low-probability (HILP) events, which are often region- and time-specific and carry substantial interruption costs. Strategies to enhance resilience can be preventive, corrective, or recovery-oriented, each with the aim of reducing the duration and severity of outages [4].

Several studies have analysed real-world HILP events to develop and validate resilience metrics and models. For example, the August 2020 storm in Iowa caused approximately USD 11 billion in damages and affected over one million customers [5]. Severe storms and floods in Brazil—including the July 2020 cyclone, the November 2023 São Paulo storm (which left 2.5 million people without power), and the April 2024 floods in Rio Grande do Sul (which displaced over 580,000 inhabitants and damaged 200,000 homes)—were investigated in [6, 7]. In Germany, a topographic assessment identified flood risks to medium-voltage (MV) substations, highlighting vulnerabilities related to surface runoff and localized sinks [8], while heavy rainfall scenarios were simulated using real data from a German distribution

system operator (DSO) [9]. These studies demonstrate the critical importance of resilience for the planning, operation, and maintenance of power systems. As can be seen, the authors often focus on cases of extreme weather conditions. However, these are not the only causes that can be classified as HILP events. Another major events may arise from unintentional or intentional human intervention, such as terrorist and cyber attacks [10]. Major disruptions may cause cascading failures, which are faults spreading through the network after outage of one or more components. Cascading failures often originate from unexpected shutdowns [11], element overloading, malfunction, or failure. The latter cases are especially relevant for meshed networks, where power flow redistributions gradually disable network components from operation.

1.1 | Resilience Quantification

Despite general consensus on the importance of resilience, its quantification remains challenging due to the absence of standardized metrics. Current approaches include performance metrics, system-level indices, and geographical analyses. For instance, a data-driven method that estimates the risk of large events based on historical outage data, quantifying both the probability of high-cost outages and the benefits of resilience investments, is proposed in [5]. In [12], a holistic resilience index was introduced considering diversity, redundancy, subsidiarity, and storage capacity in low- and medium-voltage networks. Spatial resilience assessments incorporating hazard and vulnerability layers using GIS methods were applied in [13]. The use of condition and health indices for maintenance planning, despite their limited predictive capability, was critically reviewed in [14].

Another proposed resilience measure is the grid strength, related to the short-circuit level, which is particularly relevant for systems with increasing penetration of inverter-based resources that minimally contribute to the short-circuit current [15].

Comprehensive reviews of resilience metrics are provided in [16]-[17]. Although the applied indices vary, [16] emphasizes that the metrics should capture three key attributes: threat, likelihood, and consequence. A widely used conceptual tool is the resilience trapezoid (Figure 1), which illustrates system performance, degradation and recovery during HILP events.

In [1], resilience is quantified using the following metrics: expected maximum load loss $\mathcal{L}$, expected load interruption rate $\mathcal{S}$, expected automatic restoration time $\mathcal{T}^{\mathrm{rs}}$, expected load restored by automation $\mathcal{L}^{\mathrm{rs}}$, expected repair time $\mathcal{T}^{\mathrm{rp}}$, and expected energy not supplied (EENS). These are calculated using Equations (1)–(6)

$$\mathcal{L} = \sum_{s\in S} \pi_s \left(R_{0\mathrm{o}} - R_{\mathrm{pdi}}\right), \tag{1}$$

$$\mathcal{S} = \sum_{s\in S} \pi_s \left(\frac{R_{0\mathrm{o}} - R_{\mathrm{pdi}}}{t_s^{\mathrm{i}} - t_s^{\mathrm{m}}}\right), \tag{2}$$

$$\mathcal{T}^{\mathrm{rs}} = \sum_{s\in S} \pi_s \left(t_s^{\mathrm{d}} - t_s^{\mathrm{m}}\right), \tag{3}$$

$$\mathcal{L}^{\mathrm{rs}} = \sum_{s\in S} \pi_s \left(\frac{R_{\mathrm{pdo}} - R_{\mathrm{pdi}}}{R_{0\mathrm{o}} - R_{\mathrm{pdi}}}\right), \tag{4}$$

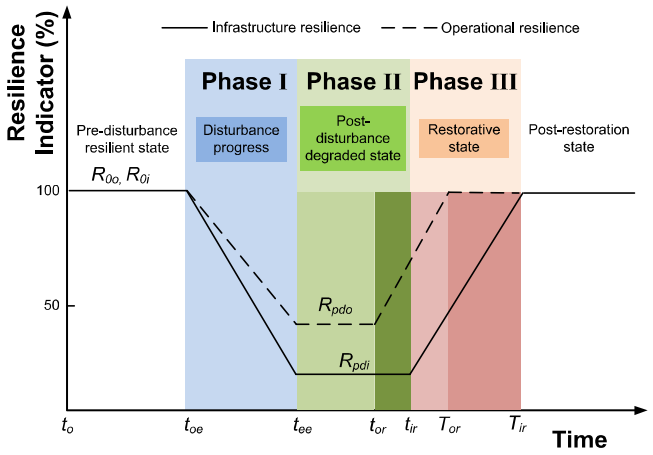

FIGURE 1 | Conceptual resilience trapezoid [18].

$$\mathcal{T}^{\mathrm{rp}} = \sum_{s\in S} \pi_s \left(t_s^{\mathrm{r}} - t_s^{\mathrm{d}}\right), \tag{5}$$

$$\mathrm{EENS} = \sum_{s\in S} \pi_s \int_{t_s^{\mathrm{i}}}^{t_s^{\mathrm{r}}} \left(R_{0o} - f_s(t)\right)\mathrm{d}t, \tag{6}$$

where S denotes the set of outage scenarios, s represents each scenario, π_s is the probability of equipment failure, and t and R correspond to the time and resilience indicator defined in Figure 1.

Additional commonly used metrics are summarized under the acronym F.L.E.P. ($\Phi\Lambda E\Pi$), which assesses how fast (F) and how low (L) the resilience drops during a disturbance, how extensive (E) the degraded state is, and how promptly (P) the system recovers [19].

Despite ongoing research, resilience quantification remains an open issue, with different metrics and frameworks applied depending on system type and application context. Notably, all the described approaches use in their initial phase (Phase I in Figure 1) the concept of preserved load to characterize system performance during disturbances. This quantity also serves as the basis for the resilience assessment presented in this study, a detailed explanation is provided in Section 2.4.

1.2 | Specifics of Meshed Network Operation and Resilience Challenges

Resilience is also a critical aspect for meshed distribution networks, predominantly used in MV and LV systems within densely populated urban areas. These networks typically employ underground cables, providing natural resilience against extreme weather and physical damage. Given their role in supplying critical infrastructure and essential services, they require exceptionally high reliability and resilience. From another point of view, meshed networks, stretching in a relatively small geographic areas, are less affected by localized climatic phenomena relevant to wide-area distribution networks. If a natural disaster impacts the area, the entire meshed network is likely to be affected simultaneously.

However, the meshed topology introduces significant operational complexity for DSOs [20, 21]. As a result, this topology is rarely used in practice and is underrepresented in research. Despite the inherent robustness and compliance with common N-1 and N-2 design criteria, these networks may not perform well under extreme HILP scenarios involving multiple simultaneous failures. Meshed distribution networks are particularly vulnerable to cascading failures, often triggered by a single fault followed by overloading, fuse failures, protection relay tripping, or overvoltages. This risk is particularly pronounced at the LV level, where DSOs often lack comprehensive monitoring and control of individual network elements. Such cascading processes can escalate unpredictably, potentially compromising the entire network. While cascading failure resilience has been studied extensively in transmission systems [22, 23], there is limited research addressing MV/LV distribution networks, which have substantially different operational characteristics.

Options for improving resilience in such networks are limited. While topology modifications could enhance resilience, they are difficult to implement and their benefits are challenging to evaluate. Practical improvements typically focus on strengthening individual components, while considering economic feasibility.

1.3 | Paper Aim and Structure

This study investigates the resilience of a specific, extensive meshed MV/LV network located in an urban area [24]. Although the network's topology and robustness suggest high reliability, this does not guarantee resilience to HILP disturbances. The most significant threat is considered cascading failures, where progressive overloading of network elements can lead to widespread outages. In Section 2, the paper first presents the methodology, including assumptions and simulation processes used to evaluate network performance over 1 year of operation. The analysis focuses on identifying the network's weakest elements and suitable measures for resilience enhancement.

The results (Section 3) brings findings from the annual operation analysis, supplemented by an in-depth examination of a critical network state – the annual peak load (Section 3.2). The study then explores potential mitigation measures and resilience improvement strategies (Section 3.4), applied and evaluated across the full year of operation. Finally, the paper discusses the overall network performance, assesses the impact of individual mitigation measures on resilience, and outlines future research directions for resilience assessment and improvement in meshed networks (Section 4).

2 | Methodology

The method of resilience analysis is proposed for a dense-meshed LV distribution network, whose operation is entirely dependent on the supplying feeders from the substation. Usually, in the city-centers, where meshed systems are deployed, alternative supply paths and distributed energy resources (DERs) are not available. Such situation is applicable to relevant network under test [24]. Therefore, the most exposed and critical elements of subjected network are the MV feeders connected directly from the supplying HV/MV substation. Major events near the substation causing outages of the supply feeders may severely disrupt the network operation. Simulation of such outages, complemented with cascading failure scenarios, using a numerical model form the basis of this analysis. The resilience is assessed only with regard to the disturbance stage including prevention measures from cascading failures. The restorative stage of the disturbance is not modelled and evaluated. The simulations are conducted in Matlab environment (own code) and are based on load flow (LF) analysis. Given the number of required calculations, the node voltage method is used, allowing the low-flow problem to be solved as a linear task.

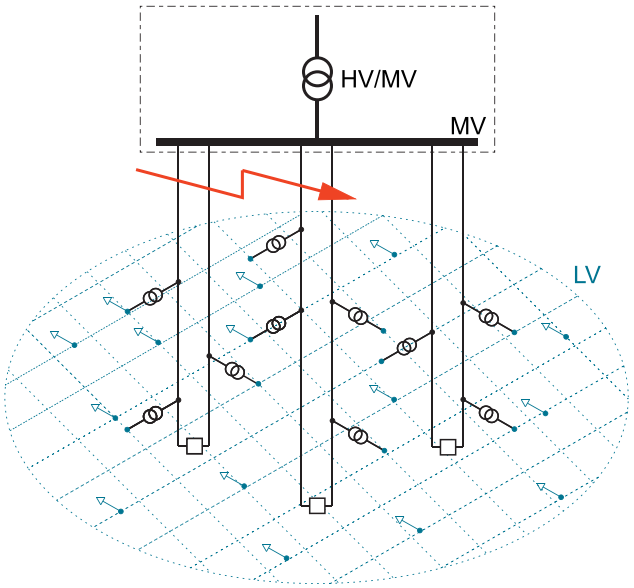

FIGURE 2 | Simplified diagram of MV/LV meshed network.

2.1 | Meshed Network Description

Simulations in this study were performed on the aforementioned network model, published in [24]. The simplified diagram is shown in Figure 2, where also an example of a four-feeder outage is indicated. From the MV side, the network contains six radial branches, to which are connected both MV customers and, mainly, 79 distribution transformers (DT), which feed the LV meshed network. These are located in distribution transformer stations (DTS), either individually or in pairs. In the latter case, they can operate in parallel by switching on the LV bus couplers, which connect the LV nodes of both DTs. A majority of customers are connected to a meshed LV system, making the load in that part of the network predominant. Due to the meshed topology of the LV network, most loads can be supplied via multiple paths, providing a level of redundancy. The network comprises 1424 LV lines and 1197 LV nodes. The issue of the LV lines topology has been addressed and published in [25]. The DTs are equipped with upstream active power protections (UAPP), which disconnect the DT from operation in cases when a fault occurs at MV level. This measure is necessary in the fault isolation process to avoid feeding the fault through the LV grid. The UAPP function and setting optimization in the relevant network is discussed in [20]. Distributed energy resources are not considered.

2.2 | Outages Scenarios

In the presented study, all possible combinations of MV feeder outages were simulated to assess grid resilience. Given the total number of six MV feeders, the number of combinations is given by Equation (7), where NoLF stands for number of lost feeders.

$$C = \sum_{\mathrm{NoLF}=1}^{5} \binom{6}{\mathrm{NoLF}} = 62, \tag{7}$$

Therefore, the total of 62 cases were considered for simulations. These cases are further grouped by NoLF and hence denoted as N-NoLF. The example of a N-4 outage case is indicated in Figure 2 with a lightning icon. It should be noted that both the MV and LV network parts offer numerous reconfiguration possibilities. In this study, the calculations were performed using the default network configuration, with the bus couplers switched off in the transformer stations.

To analyse the network behaviour under varying load conditions, all outage combinations were simulated using generated load datasets that reflect a full-year network operation. These datasets were derived from available historical data of total year customers' consumptions and standardized load profile curves varying for different consumer character. This way, the total energy consumption is spread out with assigning each hour with active power, whereas the reactive power is calculated using constant power factor of 0.99. These were complemented with measured wholesale consumption, mostly connected to the MV part of the network. By combining the available data, hourly load values were assigned to each consumption node throughout the year. As a result, for each of the 62 outage combinations, the simulations can be run 8760 times with varying load input. In all simulations constant slack voltage of 1.036 p.u. is assumed.

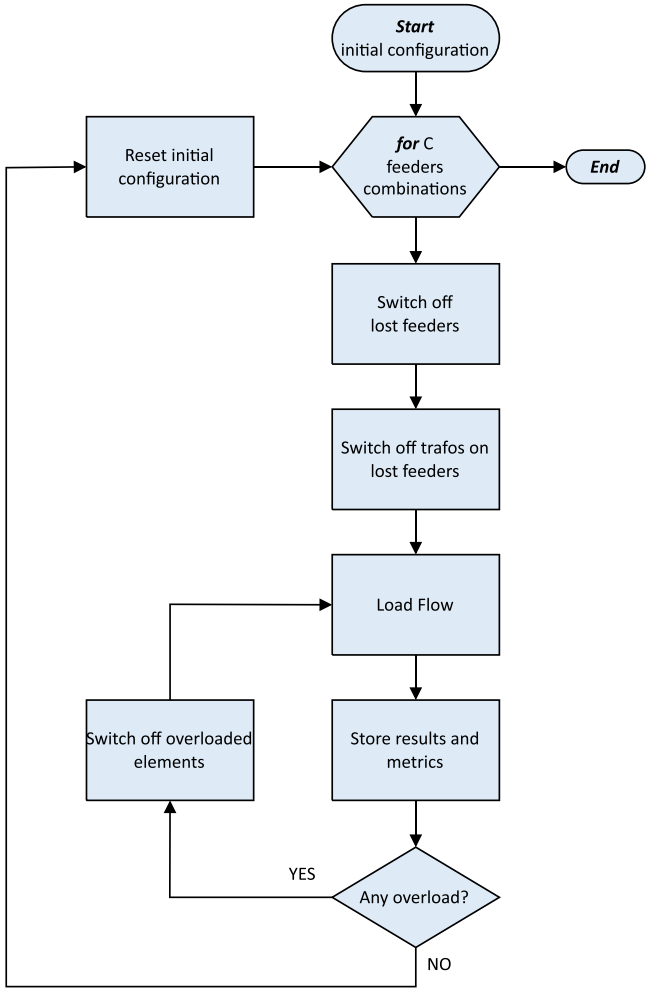

FIGURE 3 | Simulation flowchart.

2.3 | Cascading Failure

Feeder outages inevitably cause power flow redistribution in the meshed network, potentially overloading certain elements that are then automatically disconnected from operation. This can trigger further overloading and consequently a cascading failure. It is difficult to estimate the time scale of cascading failure propagation as it depends on detailed setting of protections, condition of cables and fuses, dynamic effects etc. This paper is limited to assessing each step of cascade as a separate steady state ignoring the time-scale of the event impact. The flowchart of disturbance simulation including cascading failure is shown in Figure 3. The diagram reflects the whole set of feeders combinations, where the outages for each case are considered to be simultaneous. Following the feeders outage, the UAPP function is emulated by switching off all the DTs connected to lost feeders. This action disconnects customers which are supplied radially from the lost feeders. The rest of the loads are supplied through the rest of the feeders and LV grid with redistributed power flows. Therefore, the LF is calculated and checked for operation constraints, from which loading of DTs and lines are critical for starting the cascading failure. The overloaded elements are then disconnected (emulating fuses, circuit breakers) and the process is repeated until no element is overloaded. The operation constraints were considered as maximum loading of both lines and transformers as 100% and voltage limits as 0.9 and 1.1 of nominal value. The meshed topology is very resistant to voltage events, so the voltage-constraint violations are not relevant to this case study. The whole process depicted in diagram in Figure 3 is repeated for each variant of load setting, representing each hour within the year operation simulation.

2.4 | Resilience Evaluation

Since the unknown timescale of simulated cascading failures, the analysis is focused only on how low the resilience falls. The study does not deal with the duration of the disturbance or the time of system recovery. In order to monitor the L of the FLEP listed metrics, the resilience indicator was defined as the amount of preserved load, that is the amount of load supplied to consumers in the degraded state. To allow comparison across different load settings during the simulated year of operation, the preserved load is expressed as a relative value to total served load in the pre-disturbance state. The Λ is calculated as given by equation (8), where R_0 is the initial served load (pre-disturbance) and R_{pd} is the preserved load in post-disturbance state when the cascading effect stops.

$$\Lambda = \frac{R_{\mathrm{pd}}}{R_0}, \tag{8}$$

The Λ is calculated for each simulated hour and each outage combination. Besides the Λ metric, supplementary information are stored for each simulated case allowing further investigation of the disturbance process:

- whether the outage case lead to cascading failure (Yes/No),
- number of lost lines during the disturbance,
- number of lost transformers during the disturbance.

To obtain the statistics about the most frequently overloaded elements, for each line and DT an information about the number of overloads is cumulatively stored. This is also supplemented with storing the cascade step in which each element got overloaded.

2.5 | Weakest Elements Identification and Resilience Improvement Measures

The identification of key elements is another subject which could be looked on from several aspects, and resilience related study is presented, for example in [23]. In a previous study, the weakest element in the network was determined based on the disconnected power in the area resulting from the failure of the given element [26]. Calculation results can lead to identification of key infrastructure elements that need to be improved, and appropriate corrective actions.

Specific to the meshed network topology and considered disturbances scenarios, the weakest elements are identified based on conducted cascading failure simulations and statistical evaluation of all cascades. By analysing results from all feeder outage simulations, the most vulnerable elements—lines and DTs—are identified as the most frequently overloaded. The selection of such selected weakest elements is further narrowed down by focusing on those elements, which happened to get overloaded most frequently in the first step of the cascading failure and therefore initiated the cascading effect in the first place. Strengthening those elements could prevent from cascading failures propagation and overall improve the resilience indicators.

Given the previously mentioned aspects of network operation, it is clear that the network complexity results in an enormous number of possible configurations and reinforcements, making it very challenging to optimize the operation cost-effectively. At the same time, the number of measures that can be applied to increase resilience is limited. By identifying the key elements (lines and DT) that are most often overloaded, the proposed measure is to reinforce these elements. From a practical point of view, this may involve installing additional lines (doubling existing ones) or replacing DTs with ones of higher nominal power rating. Another viable measure is network reconfiguration, specifically modifying the LV side interconnection by switching on the bus couplers.

3 | Simulation Results

According to the principles described in the Methodology, the outages simulations were performed for each hour of 1 year, that is, 8760 unique load combinations. This simulation setup yields

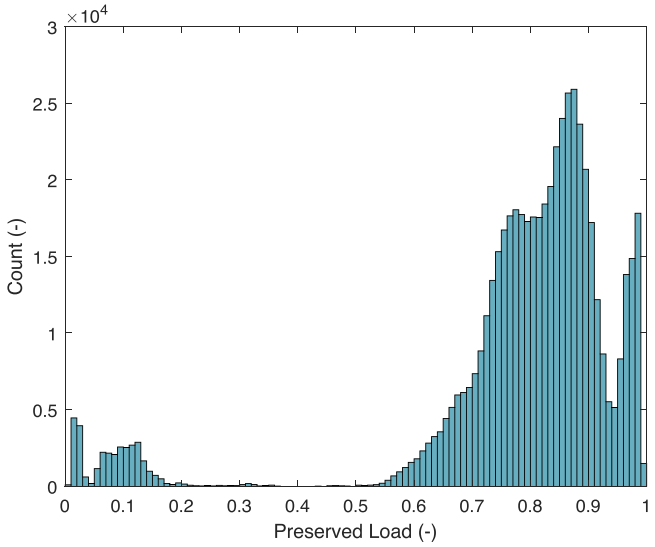

FIGURE 4 | Histogram of preserved load across all simulated cases.

62 × 8760 = 543,120 simulated cases. Some of the cases lead to cascading failure propagation, requiring additional load flow calculations of each cascade step.

The results include several main aspects:

- statistical evaluation of the resilience metrics during simulated 1 year operation,
- detailed analysis of disturbances during annual maximum load,
- weakest elements identification based on simulated 1 year operation,
- assessing resilience improvement after applying corrective measures.

3.1 | Statistical Resilience Assessment

Any of the MV feeder outages simulation leads to losing served load in the network as the affected feeders are isolated from the network and thus radially supplied customers from these feeders are also disconnected. The more severe drop in served load occurs in situations when the disturbance causes overloading and develops into cascading failure. From the set of 543,120 simulated cases, only 36,814 of them developed into cascading failure implying solid network resilience to such outages. Naturally, most cascading failures relate to situations with highly loaded network state and multiple feeder outages. The distribution of relative preserved load (Λ) across the whole dataset is shown in histogram in Figure 4. It shows that majority of simulated disturbances lead to inconsequential decrease of served load peaking in the range of 0.8–0.9. The histogram also clearly highlights the difference between disturbances that lead to cascading failures ($\Lambda < 0.4$) and those that do not ($\Lambda > 0.4$).

The overall representation of combinations of outages is split into five groups, according to number of lost feeders NoLF (from 1 to 5). The distribution for separate N-NoLF groups is depicted

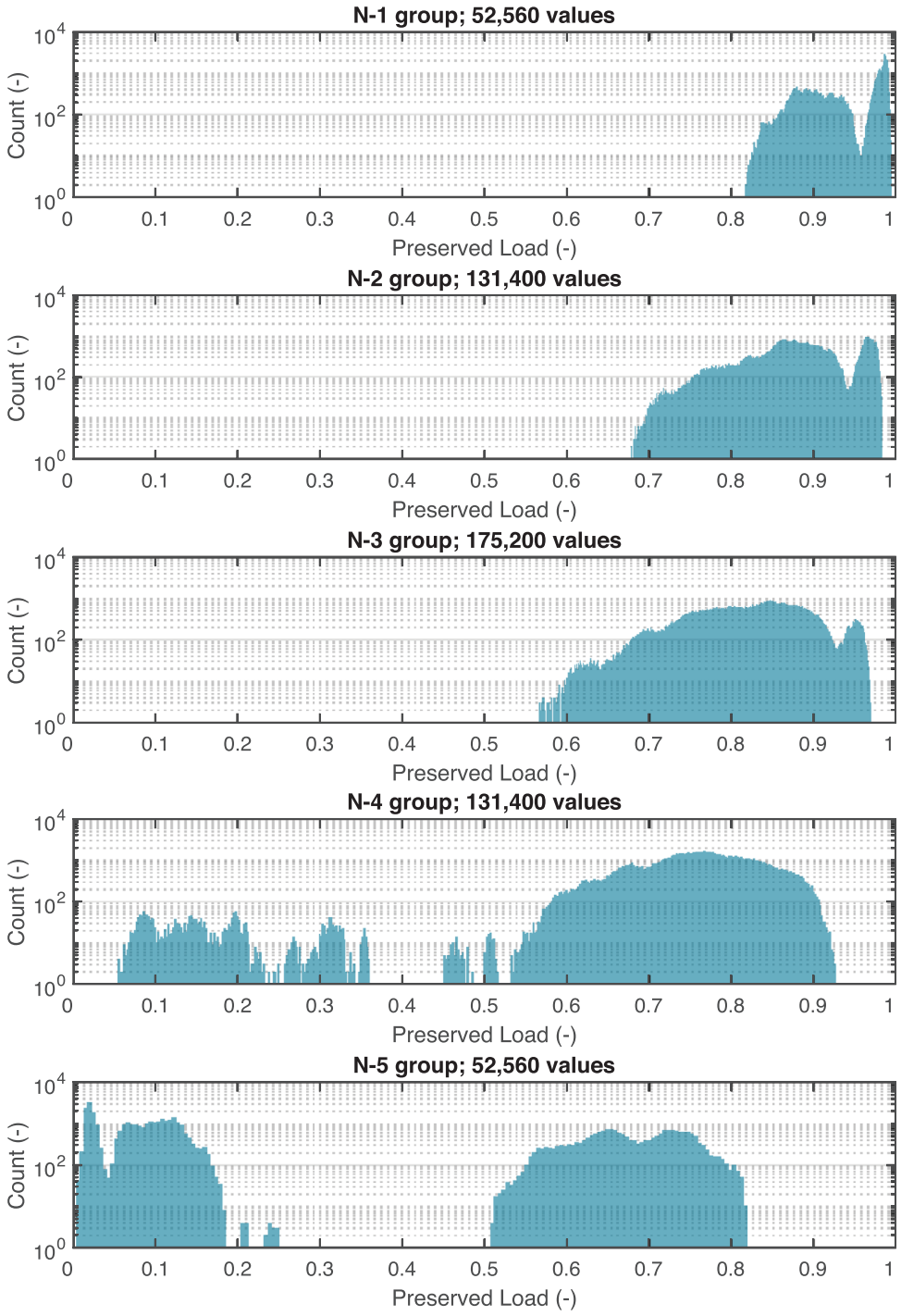

FIGURE 5 | Histogram of preserved load by each NoLF group, *y*-axis is in logarithmic scale.

in Figure 5, where for better readability, a logarithmic scale is applied. The histograms confirm a clear dependence of preserved load on the number of affected feeders, with a noticeable shift in the distribution spectrum. In addition, it is apparent that cascading failures do not occur until the outages of four feeders. This fact highlights great resilience of subjected network to similar disturbances. For outages of five feeders, the network operation is becoming critical (the whole network is fed from one feeder), in which case there is a significant risk of outage of the last feeder and entire blackout of the system. In view of these facts, the cases of loss of four feeders (N-4) were identified for further assessment, with possible relevant resilience improvement by adopting mitigation measures.

The cumulative number of overloads for each branch element across all N-4 outages combinations during the year operation is depicted in histograms in Figures 6 and 7. The elements on the *x*-axis are primarily sorted by the frequency of overloads in the initial step of cascading failures, and secondarily by their total number of overloads. The initial (first) cascade step is differentiated from the latter stages with blue colour and relatable columns are bordered with the vertical dotted lines. The

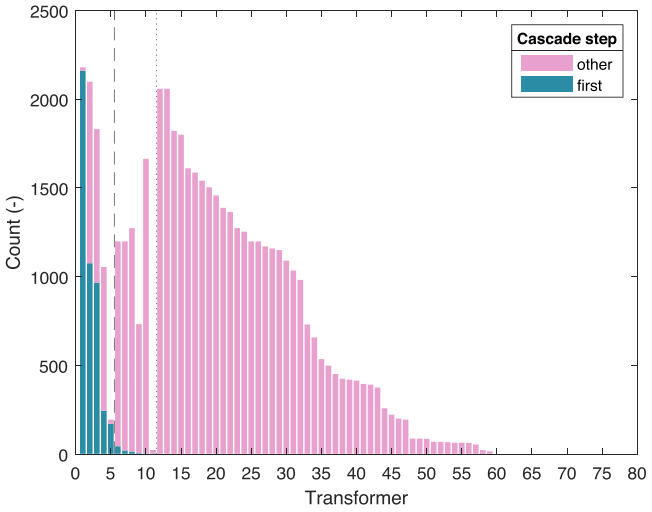

FIGURE 6 | Histogram of overloads of individual transformers (sorted).

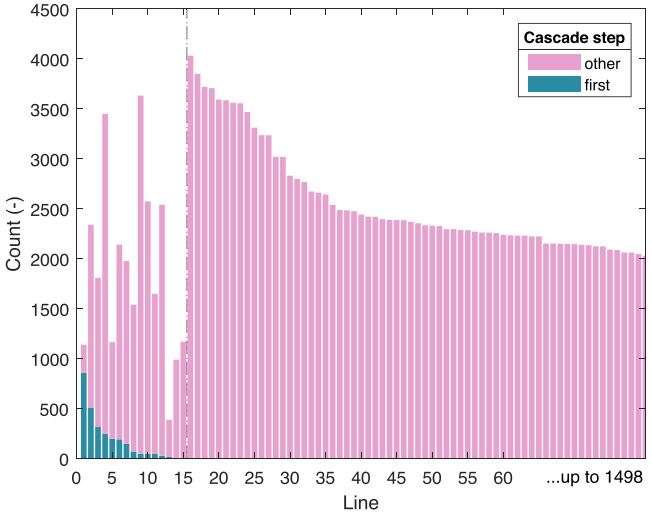

FIGURE 7 | Histogram of overloads of individual lines (sorted).

Figure 6 shows that very few transformers (11) are repeatedly overloaded in the initial cascade step, which serves well for bottlenecks identification. Only a small number of transformers (approximately 20) experience no overloading during cascading failures. The Figure 7 shows only first 80 of sorted lines (out of 1498) for better readability. In the whole picture, approximately half of the lines (701) experience some overloading across the simulations. Repeated overloads in the first cascade step is found with 15 lines.

3.2 | Detailed Disturbance Analysis

From the 8760 simulated hours, the one with maximum total served load was chosen for more detailed analysis. Closer examination of the disturbances progress is depicted in Figure 8 with the aid of resilience trapezoid concept, introduced in Figure 1. Individual curves represent each of the 62 cases and are differentiated with colour respective to each NoLF group.

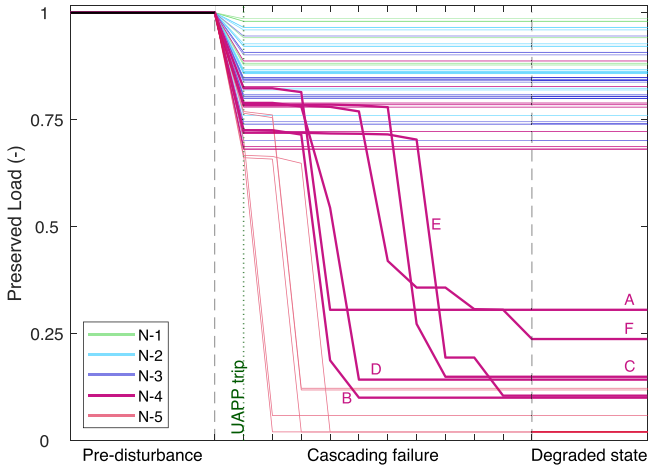

FIGURE 8 | Preserved load during disturbance simulations.

TABLE 1 | Average values of Λ for each NoLF group.

NoLF	1	2	3	4	5
Λ_{avg} (-)	0.94	0.88	0.82	0.52	0.06

It can be seen that most of the cases do not lead to cascading failure and the network gets stabilized after the UAPP trip (dotted vertical line), which has isolated only MV and radially supplied customers. These include all N-1, N-2, N-3, and most of the N-4 combinations when at least two thirds of the load preserved. Six of the N-4 cases (highlighted in Figure 8) suffered from severe cascading failure, as did all of the N-5 cases. The results of Λ metric are in Table 1, where each NoLF group is represented by mean average value of Λ_{avg}.

Figure 8 supports previous claims about network behaviour, proving good resilience even up to three lost feeders, whereas in the case of losing five feeders, the network almost inevitably leads to significant drop of served load and cannot be effectively supplied only from one feeder. Also, the potential for improvement lies mostly with N-4 cases from which six instances (labelled A–F) that resulted in cascading failures were selected for closer examination.

Table 2 simplistically shows the procedure of cascading failure for these selected instances. Individual rows represent cascade steps and columns denote cases A–F for lines and transformers. The table shows count of overloaded elements in each step. It could be concluded that the initial step of cascading failure does not always dispose with large number of overloaded elements. For example, in instance C, only one overloaded line following the feeder outage initiates a cascade effect that leads to a loss of substantial amount of load.

3.3 | Weakest Elements

The identification of weakest branch elements is based on the histograms in Figures 6 and 7. The most frequently overloaded elements in the first cascade step were selected as the weakest and suggested as subjects to corrective measures. These are also

TABLE 2 | Number of overloaded elements of during cascading failure simulation for selected cases A–F with severe resilience drop.

Casc.	Case A		Case B		Case C		Case D		Case E		Case F	
step	Line	Trafo	Line	Trafo	Line	Trafo	Line	Trafo	Line	Trafo	Line	Trafo
1	***4***	***3***	***2***	***4***	***1***	***0***	***3***	***2***	***0***	***1***	***1***	***1***
2	33	6	33	7	1	0	21	6	0	1	0	1
3	145	4	199	6	2	1	113	9	4	1	7	3
4			18	0	5	3	123	5	6	1	25	4
5					14	6			11	2	118	5
6					105	8			40	4	20	1
7					12	1			172	8	1	0
8									1	1	8	1
9									29	0	2	0
10											7	0

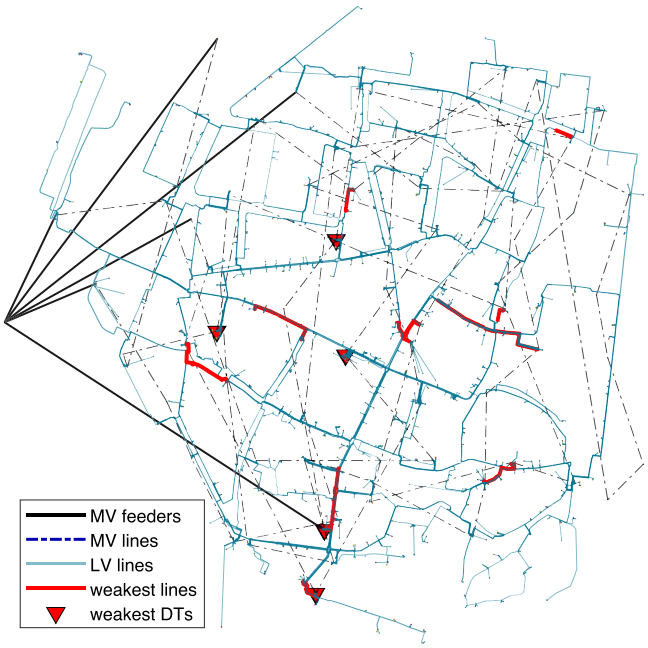

FIGURE 9 | Extensive meshed network diagram with highlighted weakest links.

bordered with the dashed vertical line. Among the distribution transformers, only the top five were identified as the weakest, each experiencing over 100 overloads during the year-long simulation. This limited selection also reflects economic considerations. On the other hand, due to the lower costs associated with reinforcing cable lines, all 15 lines that experienced any overloads in the initial step of the cascade were identified as the weakest. The weakest elements are also highlighted in Figure 9 where spatial network diagram is shown.

3.4 | Network Resilience Improvement

Due to the high complexity of the network, it is not possible to easily evaluate the effect of reconfiguration of feeders (on MV side) on improving both reliability and resilience; it is necessarily a very complex optimization task, out of the scope of this paper. However, focusing only on N-4 scenarios and the identified weakest elements, several straightforward measures for improving resilience were designed, including reinforcing the bottlenecks and reconfiguring the LV grid. Four simple measures were chosen for the case study:

1. doubling of weakest lines (measure M1),
2. increasing the rating of weakest DTs (M2) (from 630 kVA to 1000 kVA),
3. switching on all LV bus couplers (M3),
4. combining the above three measures (M123).

First two measures are focused only on the identified weakest elements of N-4 cases, that is top 15 weakest lines and top five weakest transformers. The doubling of lines (M1) was carried out as decreasing the line impedances and increasing their ampacities. The replacing of DTs (M2) was simulated as increasing the nominal power and also its short-circuit impedance by 1%. The LV reconfiguration (M3) involves interconnecting LV busbars of parallel DTs and therefore leads to enhanced complexity of meshed system. By default, these couplers are disconnected as the bus-splitting decreases level of fault currents in the network [27].

After incorporating abovementioned measures, the simulations of all cases were repeated, that is the whole year of operation combining with all possible feeder outage combinations. This required running additional $4 \times 543{,}120$ simulations. The results of such simulations are concluded in Table 3. The table first lists the number of cases that resulted in cascading failures. As already shown in Figure 5, the results show that all cascading failures occurred only in N-4 and N-5 scenarios. From the total of 36,814 cascading failure occurrences only 5573 cases belong to N-4 group meaning that most of the four-feeder outages combinations do not lead to cascading failure propagation. The most significant reduction in cascading failure probability was achieved through measure M3, that is switching on all LV bus couplers, and, naturally, through the combined measure M123.

TABLE 3 | Comparison of network performance for resilience improvement measures.

Measure	None	M1	M2	M3	M123
Number of cases which lead to cascading failure					
Total	36,814	35,014	33,683	25,837	21,165
N-4 & N-5	36,814	35,014	33,683	25,837	21,165
N-4	5573	3939	3048	1477	157
$\Lambda_{meanavg}$					
Total	0.7824	0.7835	0.7885	0.7923	0.7970
N-4 & N-5	0.6297	0.6329	0.6476	0.6587	0.6728
N-4	0.7471	0.7502	0.7580	0.7565	0.7620
Λ_{median}					
Total	0.8273	0.8273	0.8274	0.8274	0.8276
N-4 & N-5	0.7328	0.7339	0.7380	0.7398	0.7417
N-4	0.7612	0.7620	0.7643	0.7647	0.7656

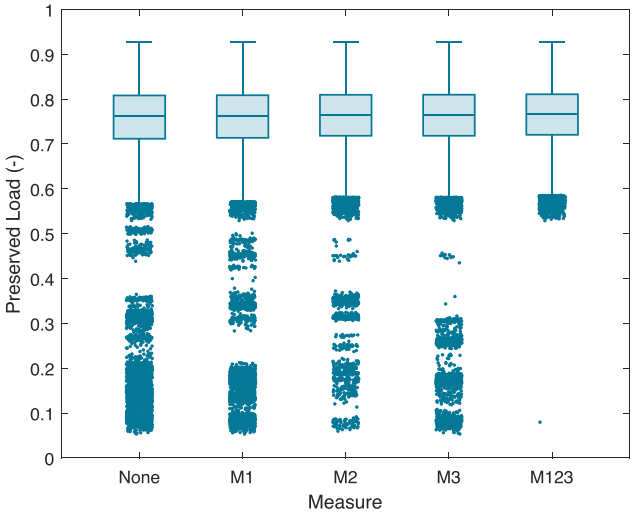

FIGURE 10 | Distribution of preserved load for all N-4 scenarios across corrective measures.

Table 3 also presents the Λ metrics for all computed combinations demonstrated as both mean values and medians. The results indicate that the metric improvement is not significant, especially when accounting with all outage combinations. These improvements become more apparent when focusing only on N-4 and N-5 groups, where the applied measures prevent from cascading failure propagation in some cases, and therefore increase the preserved load. Despite that, the resilience improvements remain minor when viewed through mean average and median values.

The statistical distribution of Λ metric across individual corrective measures is better shown using boxplot in Figure 10. This figure only presents reduced dataset to only N-4 group (131,400 cases), which were identified for resilience enhancement. In the boxplot visualization, the central box represents the interquartile range (25th to 75th percentile); with the median indicated by a line inside the box. The whiskers extend up to 1.5 times the interquartile range in both directions. Jittered dots denote outliers – values that occur with low probability.

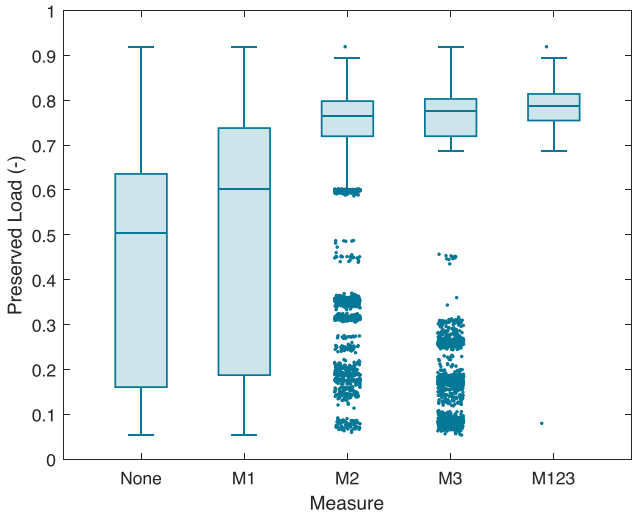

FIGURE 11 | Distribution of preserved load for N-4 scenarios leading to cascading failures across corrective measures.

Comparing the boxplots for each improvement measure, the distribution of Λ metric is very similar, mostly differing only in outliers distribution. The interquartile range and median show minimal variation, consistent with the last row of Table 3, where Λ differs only in the third decimal place. Most cases leading to cascading failures are represented as lower outliers, reflecting the minority of all simulated scenarios. The distribution of outliers also highlights the severity of the worst-case resilience drops. Overall, the resilience improvement of applied measures is not significant.

The effect of improvement measures is better displayed in Figure 11, where the dataset is narrowed down to those N-4 cases that caused cascading failures (prior to applying corrective measures), that is the 5573 cases from Table 3. It is evident that individual measures shift the Λ distribution towards higher values, as indicated by the rising median from left to right in the figure. Also, measures M2, M3, and M123 enhance the distribution by narrowing the interquartile range. This figure clearly shows the improvement of Λ reached by applying all of identified measures. The lowest impact is achieved by doubling top 15 weakest lines (M1), the biggest impact is achieved by applying the combined measure M123, where only one cascading failure (one outliar) leads to severe resilience drop. Measures M2 and M3 lead to similar distribution, where M3 achieves higher median value but more outliers lead to larger resilience drop.

The impact of individual corrective measures for selected simulation sample for annual load maximum described in Section 3.2 is presented in Figure 12 allowing a closer look on the disturbance process. Individual curves represent mean average values of served load across all N-4 cases with different applied measures.

The values of Λ_{avg} metric for individual measures are also in Table 4. The results show, that the reinforcement of selected lines (M1) has but little effect on resilience in this load setting. This is because newly installed lines affect the impedance relations and

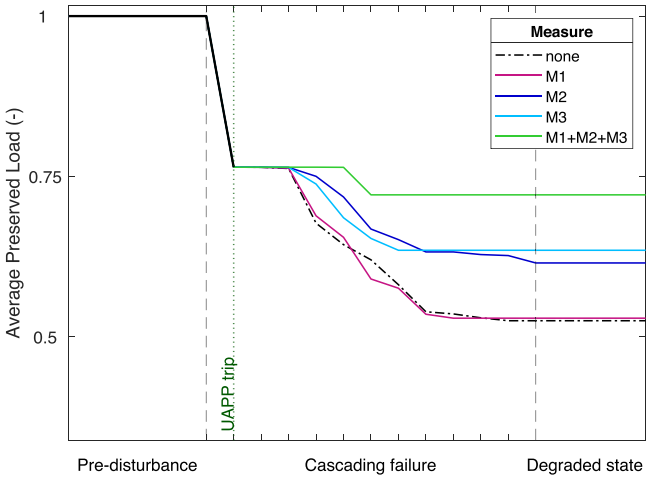

FIGURE 12 | Average preserved load in N-4 cases with applied measures (selected scenario).

TABLE 4 | Average values of Λ for applied measures to N-4 cases.

Measure	None	M1	M2	M3	M123
Λ_{avg} (-)	0.52	0.53	0.62	0.63	0.72

the power flows redirect so that other elements are overloaded and cascading failures evolve nevertheless. The reinforcement of top 5 weakest transformers (M2) lead to notable resilience improvement; however, replacing these transformers may not be practical or cost-effective solution. Similar improvement is achieved by interconnecting the bus couplers in transformer stations (M3). This measure requires no investment costs but is not desired from the fault current level point of view. The greatest improvement would be achieved by employing the combined measure M123. Overall, the findings from the detailed case analysis comply with the distribution from year simulations shown in Figure 11.

4 | Conclusion

This study presented a resilience analysis of an extensive meshed MV/LV network located in an urban area. The analysis focused on cascading failures triggered by extreme events leading to MV feeder outages. Resilience was evaluated based on the preserved load in the degraded network state.

All combinations of MV feeder outages (62 in total) were simulated under hourly load variations representing 1 year of operation, resulting in 8760 scenarios per combination. Additionally, four corrective measures were assessed, leading to a total of $62 \times 8760 \times 5 = 2{,}715{,}600$ disturbance scenarios. It should be emphasized that conventional methods often consider the failure of only one element, while the test scenarios in this case went up to the outage of 5 elements (out of 6). The amount of scenarios is undoubtedly vast; thanks to the simplifications and the chosen computational approach, it was possible to effectively achieve results.

The results indicate that the network maintains high resilience under up to three simultaneous MV feeder outages (N-3), with no cascading failures observed. This confirms the inherent resilience benefits of the meshed LV topology, provided that the UAPPs function correctly to isolate affected feeders and prevent MV-level loops.

Following these results, the analysis focused on N-4 scenarios, which exhibited the highest potential for resilience improvement. The most critical elements (lines and transformers overloaded in the initial cascade step) were identified and targeted by corrective measures. The analysis showed that only a limited number of elements are consistently overloaded, allowing for efficient and focused reinforcement.

Four corrective measures were designed to mitigate cascading propagation in N-4 scenarios. Although their overall impact was moderate (due to relatively low loading during most of the year) all measures contributed to improved resilience metrics. Among them, LV bus coupling provided the most substantial benefit, followed by replacement of the five weakest transformers. Doubling the top 15 weakest lines had the least effect.

Despite the low overall probability of cascading failures, their potential impact justifies consideration of reinforcement strategies. The load settings in this study were based on historical data, as demand increases over time, the risk of overload and cascading propagation is expected to grow.

Last but not least, to emphasize the importance of the presented issue, it is worth mentioning that the study was conducted on a model based on a real low voltage network. The operator of this network is already incorporating some of the presented results into the network reinforcement decisions.

Author Contributions

Vit Krcal: methodology, investigation, software, visualization, writing – original draft, resources, revision. **Jan Koudelka:** conceptualization, writing – original draft, revision. **Matej Vrtal:** writing – original draft, visualization, resources, revision. **David Topolanek:** supervision. **Petr Toman:** funding acquisition.

Acknowledgements

This publication was supported by the project "The Energy Conversion and Storage", funded as project No. CZ.02.01.01/00/22_008/0004617 by Programme Johannes Amos Comenius, call Excellent Research.

Conflicts of Interest

The authors declare no conflict of interests.

Data Availability Statement

The data that support the findings of this study are openly available in IEEE Dataport at http://doi.org/10.21227/kssw-1457, reference number [24]. Other data are available from the corresponding author, Vit Krcal, upon reasonable request.

References

1. M. M. Hosseini, A. Umunnakwe, and M. Parvania, "Automated Switching Operation for Resilience Enhancement of Distribution Systems," in

2019 IEEE Power & Energy Society General Meeting (PESGM) (IEEE, 2019), 1–5.

2. A. Gholami, T. Shekari, M. Amirioun, F. Aminifar, M. Amini, and A. Sargolzaei, "Toward a Consensus on the Definition and Taxonomy of Power System Resilience," *IEEE Access* 6 (2018): 32 035–32 053.

3. S. Kaloti and B. Chowdhury, "Toward Reaching a Consensus on the Concept of Power System Resilience: Definitions, Assessment Frameworks, and Metrics," *IEEE Access* 11 (2023): 81 401–81 418.

4. M. Panteli, D. N. Trakas, P. Mancarella, and N. D. Hatziargyriou, "Power Systems Resilience Assessment: Hardening and Smart Operational Enhancement Strategies," *Proceedings of the IEEE* 105, no. 7 (2017): 1202–1213.

5. A. Ahmad and I. Dobson, "Quantifying Distribution System Resilience From Utility Data: Large Event Risk and Benefits of Investments," *IET Conference Proceedings* 2024 (2025): 118–122, https://digital-library.theiet.org/doi/abs/10.1049/icp.2024.2578.

6. L. M. Nunes, R. B. Silva, and L. N. Reis, "Resilience of Electric Distribution Systems in Brazil: Analysis of the Regulatory Framework and the Ongoing Project in the Sector," *IET Conference Proceedings* 2024 (2025): 6–10, https://digital-library.theiet.org/doi/abs/10.1049/icp.2024.2550.

7. V. Ribeiro, J. Mello, A. Nascimento, B. Lobo, G. Martins, and L. Reis, "Technological Roadmap for Enhancing Electric Distribution Resilience in Brazil: A Framework for Classifying Extreme Weather Events," *IET Conference Proceedings* 2024 (2025): 241–245, https://digital-library.theiet.org/doi/abs/10.1049/icp.2024.2607.

8. F. Hankammer, N. Lienenklaus, M. Zdrallek, and F. Aschenbroich, "Topographical Assessment of Electrical Distribution System Vulnerability to Heavy Rainfall Events," *IET Conference Proceedings* 2024 (2025): 128–132, https://digital-library.theiet.org/doi/abs/10.1049/icp.2024.2580.

9. P.-H. Homberg, F. Hankammer, N. Lienenklaus, and M. Zdrallek, "Quantifying the Resilience of Sector-Coupled Energy Systems Based on Potential Impacts of Climate Change on the Distribution Grid," *IET Conference Proceedings* 2024 (2025): 88–92, https://digital-library.theiet.org/doi/abs/10.1049/icp.2024.2570.

10. V. S. Rajkumar, A. tefanov, J. L. Rueda Torres, and P. Palensky, "Dynamical Analysis of Power System Cascading Failures Caused by Cyber Attacks," *IEEE Transactions on Industrial Informatics* 20, no. 6 (2024): 8807–8817.

11. D. Liu, X. Zhang, and C. K. Tse, "A Tutorial on Modeling and Analysis of Cascading Failure in Future Power Grids," *IEEE Transactions on Circuits and Systems II: Express Briefs* 68, no. 1 (2021): 49–55.

12. P. Runte, A. K. Seyfried, and J. Myrzik, "Quantifying Resilience Enhancing System Parameters for Electrical Low and Medium-Voltage Grids," *IET Conference Proceedings* 2024 (2025): 157–161, https://digital-library.theiet.org/doi/abs/10.1049/icp.2024.2586.

13. M. Montalà-Palau, M. C. Mañé, and O. Gomis-Bellmunt, "Gis-Based Approach to Improve the Resilience of the Distribution Network," *IET Conference Proceedings* 2024 (2025): 138–142, https://digital-library.theiet.org/doi/abs/10.1049/icp.2024.2582.

14. J. Webb and K. Hencken, "Through a Glass, Darkly Making Sense of Condition / Health Indices," *IET Conference Proceedings* 2024 (2025): 152–156, https://digital-library.theiet.org/doi/abs/10.1049/icp.2024.2585.

15. D. Schoenwald and S. Ojetola, "Revisiting Resilience Indices," in *2022 IEEE Power & Energy Society General Meeting* (IEEE, 2022), 1–14.

16. Y. Yao, W. Liu, and R. Jain, "Power System Resilience Evaluation Framework and Metric Review," in *IEEE Power & Energy Society Innovative Smart Grid Technologies Conference (ISGT)* (IEEE, 2022), 1–5.

17. H. Raoufi, V. Vahidinasab, and K. Mehran, "Power Systems Resilience Metrics: A Comprehensive Review of Challenges and Outlook," *Sustainability* 12, no. 22 (2020): 9698.

18. M. Panteli, P. Mancarella, D. N. Trakas, E. Kyriakides, and N. D. Hatziargyriou, "Metrics and Quantification of Operational and Infrastructure Resilience in Power Systems," *IEEE Transactions on Power Systems* 32, no. 6 (2017): 4732–4742.

19. C. Vega Penagos, J. Diaz, O. Rodriguez-Martinez, F. Andrade, and A. Luna, "Metrics and Strategies Used in Power Grid Resilience," *Energies* 17, no. 1 (2024): 168.

20. V. Krcal, D. Topolanek, V. Jurak, and J. Orsagova, "A Software Tool for Setting Upstream Active Power Protection in a Meshed Distribution Network," in *2023 23rd International Scientific Conference on Electric Power Engineering (EPE)* (IEEE, 2023), 1–5.

21. V. Krcal, D. Topolanek, V. Vycital, and J. Vaculik, "Indication of Abnormal Operation Conditions in a Mesh Network Based on Data From Distributed Measurement," in *IET Conference Proceedings* 6 (2021), 1567–1571.

22. M. Noebels, R. Preece, and M. Panteli, "AC Cascading Failure Model for Resilience Analysis in Power Networks," *IEEE Systems Journal* 16, no. 1 (2022): 374–385.

23. P. Lv and Y. Wang, "Resilience Evaluation Method Considering Critical Line Identification of Cascading Failure," in *2023 6th International Conference on Energy, Electrical and Power Engineering (CEEPE)* (IEEE, 2023), 697–702.

24. D. Topolanek, *Meshed LV Distribution Network* (IEEE, 2022).

25. V. Krcal and D. Topolanek, "Fault Detection in Mesh Network Utilizing Measured Data From mv/lv Transformer Stations," in *Proc 11th Int Sci Symp Electr Power Eng ELEKTROENERGETIKA* (2022), 272–276.

26. M. Vrtal, V. Krcal, J. Koudelka, D. Krpelik, R. Fujdiak, and P. Toman, "Resilience Analysis in Medium Voltage Distribution System: Case Study," *IET Conference Proceedings* 2024 (2025): 217–221, https://digital-library.theiet.org/doi/abs/10.1049/icp.2024.2601.

27. D. Topolanek, V. Krcal, L. Foltyn, et al., "Optimization Method for Short Circuit Current Reduction in Extensive Meshed lv Network," *Int J Electr Power Energy Syst* 152 (2023).